

Study of electronic and optical properties of Boron Nitride

Rebecca Lalngaihawmi^{*1} and R.K.Thapa²

^{1,2}Condensed Matter Theory Research Group, Department of Physics, Mizoram University, Aizawl- 796 004, INDIA

Abstract

The optimized crystal structure, energy band structures, density of states (DOS) and optical properties of boron nitride (BN) was investigated using full potential linearized augmented plane wave method (FP-LAPW). The exchange-correlation potential was treated using the generalized gradient approximation (GGA). The band gap is calculated to be 4.4 eV.

Keywords: DFT; FP-LAPW; GGA; DOS; band structure; band gap.

PACS Nos.: 71.15.Mb, 71.15.±m, 71.20.±b

Introduction

Boron compounds have attracted increasing research interest over the past few years, as wide band gap semiconductors. The binary compounds BX belong to III-V semiconductor which crystallizes in zinc-blende structure [1]. These materials are of great technological interest for high-temperature, electronic and optical applications. This is due to their unique physical properties such as densities, extremely high thermal conductivities, wide band-gap and large resistivity [2]. Extensive research devoted to the physics and chemistry of BN during the last quarter century has led to great advances in understanding the properties.

The main aim of this work is to give a comparative and complementary study of electronic and optical properties of boron nitride using Full Potential Linearized Augmented Plane Wave (FP-LAPW) method. We will present here the results of calculated DOS and energy band of BN. This will be followed by results obtained for optical properties by using Kramer-Kronig relation which is also implemented in wien2k.

Computational method

In this work, we have employed the FP-LAPW method [3] within the framework of the density functional theory (DFT) [4] as implemented in the WIEN2k code [5]. The exchange-correlation potential has been calculated with generalized gradient approximation (GGA) based on Perdew *et al.* [6]. Kohn-Sham wave functions [7] were expanded in terms of spherical harmonic functions inside the non-overlapping muffin-tin spheres surrounding the atomic sites (MT spheres) and in Fourier series in the interstitial region. Inside the muffin-tin spheres of radius R_{MT} , the l -expansion of the wave function were carried out up to $l_{max}=10$ while the charge density was Fourier expanded up to $G_{max}=14$.

In order to achieve energy eigenvalues convergence, the wave functions in the interstitial region were expanded in plane waves with a cut-off of $K_{max}=7/R_{MT}$ where R_{MT} were assumed to be 2.45 a.u. A mesh point of 11000 k -points each were used to obtain 328 special k -points in the irreducible wedge of the Brillouin zone for BN. The energy convergence criterion were set to be 10^{-5} Ry. Theoretical lattice constant of BN is obtained by volume optimization [8].

Density of States

The electronic configurations of B and N are **B:** $1s^2 2s^2 2p^1$ and **N:** $1s^2 2s^2 2p^3$. We have calculated the total DOS of BN, the plot of which are shown in Figs. 1(a) and (b) respectively.

The major contribution to the total DOS is provided by the $2p$ states of N atom and $2p$ -states of B atom, with a small contribution from $2s$ -states of B atom and $2s$ -states of N atom in the conduction region as well as in the valence band region as shown in Figures 1(a), 1(b) and 1(c). Sharp peaks are observed at around 12.03 eV and 4.4 eV in the valence region and also at -8 eV in the conduction region which are mainly contributed by $2p$ -states and $2s$ -states of Boron respectively. A band gap of 4.4 eV is observed by using normal GGA method.

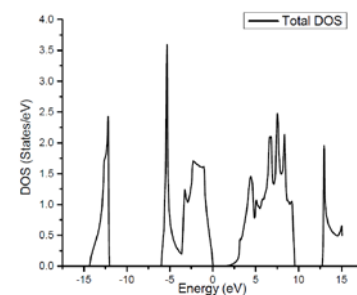


Fig. 1(a) Plot of (a) of BN atom.

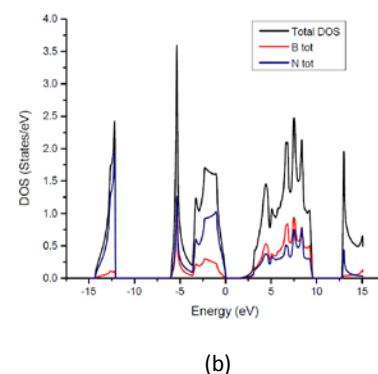
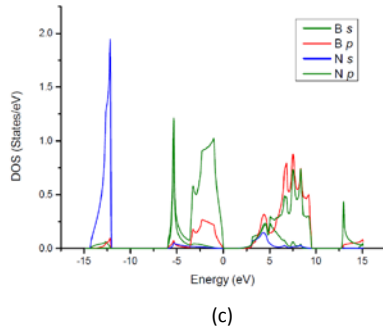


Fig. 1(b) Plot of partial DOS of BN atom


 Fig. 1(c) Plot of density of state for *s*- and *p*-states of BN atom

Band structure

For a better understanding of the electronic properties, the investigation of electronic band structure is very useful. The band structures of BN in the orthorhombic phase which was calculated and plotted on the surface of Brillouin zone by using FP-LAPW method is shown in Figure 2 respectively.

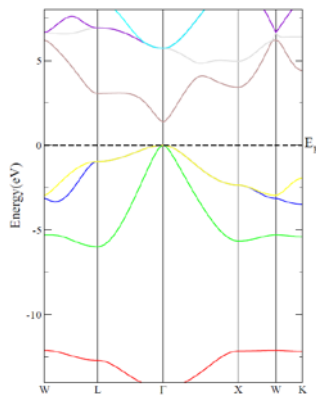


Fig. 2 Plot of band structure of BN

From the band-structure plot of BN, the core level bands were due to N-*s* state electrons followed by N-*p* state electrons in the valence region as shown in Figs. 3. At the Fermi level (E_F), N-2*p* electrons are found to be contributing, which is observed in terms of flat bands for BN. There is an indirect band gap with the maximum of the valence band lying at Γ and the minimum of the conduction band lying at X. From the band gap, it is found that the compound is a semiconductor with energy gap equal to 4.4 eV.

Optical Properties

For the calculation of optical properties, a dense mesh of uniformly distributed *k*-points is required. Dielectric function $\epsilon(\omega)$ of the electron gas depending on the frequency is important in determining the physical properties of solids. The dielectric function

$$\epsilon(\omega) = \epsilon_1(\omega) + \epsilon_2(\omega) \quad (1)$$

is known to describe the optical response of the medium at all photon energies $\hbar\omega$. The imaginary part of the

complex dielectric function $\epsilon_2(\omega)$ can be calculated using the relation

$$\epsilon_2(\omega) = \left(\frac{4\pi^2 e^2}{m^2 \omega^2}\right) \sum_{i,j} \int (i|M|j)^2 f_i(1-f_j) \times \delta(E_f - E_i - \omega) d^3k \quad (2)$$

where *M* is the dipole matrix, *i* and *j* are the initial and final states respectively, f_i is the Fermi distribution function for the *i*th state, and E_i is the energy function in the *i*th state. The real part of the dielectric function $\epsilon_2(\omega)$ can be extracted from the imaginary part by using the Kramer-Kronig relation as [9, 10]

$$\epsilon_1(\omega) = 1 \pm \frac{2}{\pi} P \int_0^\infty \frac{\omega' \epsilon_2(\omega') d\omega'}{(\omega'^2 - \omega^2)} \quad (3)$$

where *P* implies the principal value of the integral.

The optical reflectivity spectra are derived from the Fresnel's formula for normal incidence assuming an orientation of the crystal surface parallel to the optical axis using the relation [11, 12]

$$R(\omega) = \left| \frac{\sqrt{\epsilon(\omega)} - 1}{\sqrt{\epsilon(\omega)} + 1} \right|^2 \quad (4)$$

While the electronic loss-function $\left(-I_m\left(\frac{1}{\epsilon}\right)\right)$ is given by [10, 12, 13]

$$-I_m\left(\frac{1}{\epsilon}\right) = \frac{\epsilon_2(\omega)}{\epsilon_1^2(\omega) + \epsilon_2^2(\omega)} \quad (5)$$

We calculate the absorption coefficient $I(\omega)$ and the real part of optical conductivity $\text{Re}[\sigma(\omega)]$ using the following expression [9, 11]

$$I(\omega) = 2\omega \left\{ \frac{\sqrt{\epsilon_1^2(\omega) + \epsilon_2^2(\omega)} - \epsilon_1(\omega)}{2} \right\} \quad (6)$$

$$\text{Re}[\sigma(\omega)] = \frac{\omega \epsilon_2}{4\pi} \quad (7)$$

Also, the optical spectra such as the refractive index $n(\omega)$, and the extinction coefficient, $k(\omega)$, are calculated in terms of the components of the complex dielectric function as follows [11, 12, 13].

$$n(\omega) = \left\{ \frac{\epsilon_1(\omega)}{2} + \frac{\sqrt{\epsilon_1^2(\omega) + \epsilon_2^2(\omega)}}{2} \right\}^2 \quad (8)$$

$$k(\omega) = \left\{ \frac{\sqrt{\epsilon_1^2(\omega) + \epsilon_2^2(\omega)}}{2} - \frac{\epsilon_1(\omega)}{2} \right\}^2 \quad (9)$$

We have used equation (2) to equation (9) to calculate the optical properties in this study. The optical spectra calculated for the three compounds are discussed in Figures 3 to 7. The real, (ϵ_1) and imaginary, (ϵ_2)

parts of dielectric function in the energy range 0-14 eV are shown in Fig. 3 for BN compound.

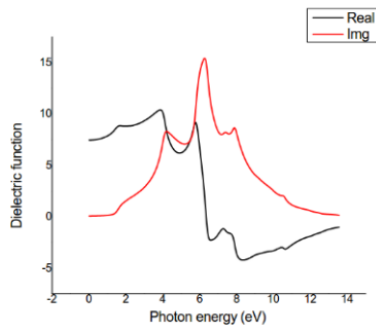


Fig. 3 Calculated real and imaginary parts of dielectric function for BN

It is interesting to note that the first peak in $\epsilon_1(\omega)$ coincides with the transition at the point L between the top of valence band and the bottom of conduction band. The major differences between the $\epsilon_1(\omega)$ spectra of the compounds appear to occur in the region where $\epsilon_1(\omega)$ is negative with BN exhibiting the least sharp structure in the region 0-14 eV. It is found that the peak intensity in the dielectric function occurs at 6 eV. This corresponds to direct interband transitions which originates from the top of the valence band at the L-point to the lowest of conduction band. In the imaginary part of the dielectric function, the onset of the absorption edge in ϵ_2 occurs at ~ 5 eV. This corresponds to optical band gap ($\Gamma_v \rightarrow \Gamma_c$).

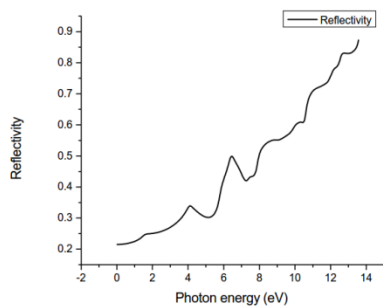


Fig.4 Calculated reflectivity of BN

In Figure 4, we exhibit the calculated reflectivity spectra for the compound using equation (4). We note that in the three compounds, the reflectivity spectra is small in the low energy region indicating that inter-band transitions do not occur at far infrared (IR) spectrum in these large band gap semiconductors but at the ultra-violet region. The behavior of the reflectivity between ~ 0 -14 eV makes the compounds particularly good for applications in visible and ultra-violet region.

The electron energy loss-function for Boron Nitride is shown in Figure 5. In this compound, the energy loss spectra exhibit a large peak at 11.32eV.

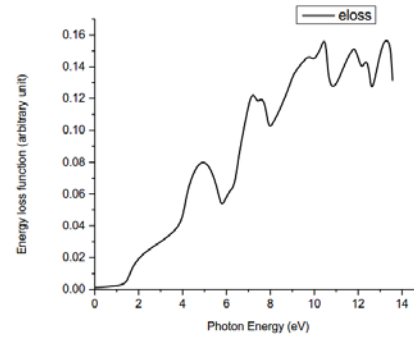


Fig 5: Calculated electron energy-loss function of BN

The calculated linear absorption spectra of BN is plotted in Figure 6. The general profiles of their frequency dependence are similar for all the compounds. For all the compounds, the onset of optical absorption involves a sharp increase in the spectra at energies corresponding to the fundamental optical gap.

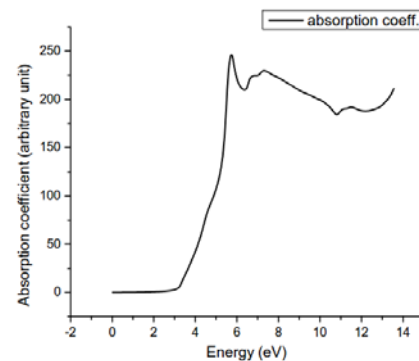


Fig. 6 Calculated linear absorption coefficient of BN

In Figure 7, the calculated refractive index and the extinction coefficient are plotted. The refractive index and extinction coefficient spectra of the compounds have resonance in the ultra-violet which corresponds to the interband transitions.

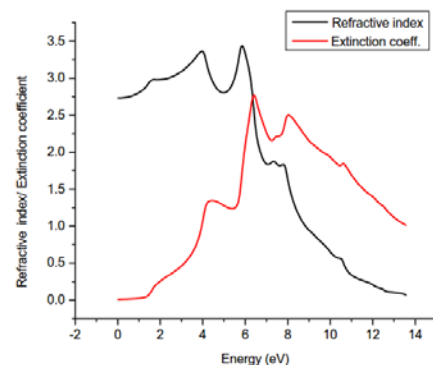


Fig. 7 Refractive index and extinction coefficient of BN

Conclusions

We have used the generalized gradient approximations in the full potential linearized augmented plane wave method to study the electronic and optical properties of zinc-blende boron mono-

pnictide BN. The binary mono-pnictides are indirect band gap ($\Gamma \rightarrow X$) compounds and are optically inactive. The value of energy gap for BN obtained for DOS and energy band calculations is 4.4 eV whereas the experimental values is 4.45 eV [15]. This means that value of energy gap obtained by GGA method is equal to experimental result. The behavior of various optical parameters like dielectric functions, refractive index, reflectivity, energy-loss function as well as extinction coefficient showed usual trends as found in other solids.

Acknowledgements

Rebecca acknowledges a MZU-UGC fellowship from Mizoram University.

References

1. D S Yadav & D V Singh, *Phys. Scr.* **85** 015701 (2012).
2. W.E. Picket, S.C. Erwin, O. Mashima, W.R. Lambrecht and B. Segall, *Diamond, Silicon, and Related Wide Gap Semiconductors (MRS Symp. Proc. No 162)* ed J T Glass, R Meissier and N Fujimori (Pittsburg, PA: Materials Research Society) (1989).
3. D.D. Koelling, B.N. Harmon, *J. Phys. C: Solid State Phys.* **10** 3107 (1977).
4. P Hohenberg, W Kohn, *Phys. Rev.* **B136** 864 (1964).
5. P Blaha, K Schwarz, G K H Madsen, D Kvasnicka, J Luitz and K Schwarz, *An Augmented Plane Wave plus Local Orbitals Program for calculating Crystal Properties: Wien2k User's Guide*(Wien: Technische Universitat Wien) (2013).
6. J P Perdew, S Burke, M Ernzerhof, *Phys. Rev. Lett.* **77** 3865 (1996).
7. W Kohn, and L Sham, *J. Phys. Rev.* **140** 1133 (1965).
8. V Heine and I Abarenkov, *Phil. Mag.* **9** 451 (1964).
9. C. Ambrosch-Draxl, R. Abt, *The Calculation of optical properties within WIEN97* (1998) ICTP Lectures Notes (unpublished).
10. Y.P. Yu, M. Cardona, *Fundamentals of semiconductors: Physics and Materials properties*, 2ndedn. (Springer-Verlag, Berlin, 1999).
11. A. Delin, A.O. Eriksson, R. Ahuja, B. Johansson, M.S.S. Brooks, T. Gasche, S. Auluck, J.M. Wills, *Phys. Rev. B* **54** 1673 (1996); P. Ravindran, A. Delin, B. Johansson, O. Eriksson, J.M. Wills, *Phys. Rev. B* **59** 1776 (1999); P. Ravindran, A. Delin, P. James, B. Johansson, J.M. Wills, O. Eriksson, *Phys. Rev. B* **59** 15680 (1999).
12. M. Fox, *Optical Properties of Solids* (Oxford University Press, UK, 2002).
13. M. Dressel, G. Gruner, *Electrodynamics of solids: optical properties of electrons in matter* (Cambridge University Press, UK, 2001).
14. Crystal Structures 1 (1963) 85-237, Second edition; Interscience Publishers, New York, New York.
15. A. Zaoui and F El Hassan, *J. Phys.: Condens. Matter* **13** 253-262 (2001).
16. R.M. Wentzcovitch, M.L. Cohen and P.K. Lam, *Phys. Rev.* **B36** 6058 (1987).
17. W. Wettleing and J. Windscheih, *Solid State Commun.* **50** 33 (1984).
18. Knittle, R.M. Wentzcovitch, R. Jeanloz and M.L. Cohen, *Nature* **337** 349 (1989).
19. D.P. Rai, M.P. Ghimire and R.K. Thapa, *Semiconductors* **48** 1411-1422 (2014).
20. Anna Delin, P. Ravindran, Olle Eriksson, J.M. Wills, *International Journal of Quantum Chemistry*, **69** 349-358 (1998).
21. F El. Hasan Haj, F. Aumane, H. Meradji and S. Ghemid, *Comput. Mater. Sci.* **50** 274 (2010).
22. A. Breidi, F El Hasan Haj, G. Nouet, S. Drablia, H. Meradji, O. Pages and S. Ghemid, *J. Alloys Compounds* **473** 80 (2010).
23. S.H. Wei and A. Zunger, *Phys. Rev.* **B37** 8958 (1988).
24. A Morita, T. Soma and T. Takeda, *J. Phys. Soc. Japan*, **32** 29 (1972).
25. T Soma, *J. Phys. C: Solid State Phys.* **11** 2669 (1978).
26. T Soma, *Phys. Status Solidi* **b119** 547 (1983).
27. R.M. Wentzcovitch, K.J. Chang and M.L. Cohen, *Phys. Rev.* **B34** 107 (1986).
28. R.M. Wentzcovitch and M.L. Cohen, *J. Phys. C: Solid State Phys.* **19** 6791 (1986).
29. M. Ferhat, A. Zaoui, M. Cartier and H. Aourag, *Physica* **B252** 229 (1998).
30. M. Ferhat, B. Bouhafs, A. Zaoui and H. Aourag, *J. Phys.: Condens. Matter* **10** 7995 (1998).
31. R.M. Wentzcovitch, M.L. Cohen and P.K. Lam, *Phys. Rev.* **B36** 6058 (1987).